Kageyama *et al. Micro and Nano Syst Lett* (2018) 6:6
https://doi.org/10.1186/s40486-018-0068-z

Micro and Nano Systems Letters

LETTER **Open Access**

Fabrication of an Au–Au/carbon nanotube-composite contacts RF-MEMS switch

Tomoaki Kageyama[1], Koichi Shinozaki[2], Lan Zhang[3], Jian Lu[3], Hideki Takaki[3] and Sang-Seok Lee[1*]

Abstract

This study aims to propose a new fabrication method for an ohmic contact type RF-MEMS switch with Au–Au/carbon nanotube (CNT)-composite contacts. These contacts are proposed to improve the reliability and the high-power handling capability of the ohmic contact type RF-MEMS switch. During the fabrication, we applied Au/CNT-composite electroplated film to the contact area in the signal line, whereas Au electroplating was used to form contacts under the cantilever of the switch. We investigated the influence of the Ar ion beam etching angle on metal layers formation and optimized the Ar ion beam etching conditions to achieve a more reliable RF-MEMS switch. We designed, fabricated, and evaluated an RF-MEMS switch to demonstrate the feasibility of our new fabrication method. We successfully fabricated an Au–Au/CNT-composite contact RF-MEMS switch; it exhibited a low insertion loss of less than 0.7 dB at frequency up to 40 GHz and a cycle life 2.7 times longer than that of an Au–Au contact switch.

Keywords: RF-MEMS switch, Au/CNT-composite layer, Reliability, Ar IBE process optimization

Background

Radio frequency microelectromechanical system (RF-MEMS) switches are considered as promising devices for use in high frequency communication modules owing to their superior RF characteristics, which include low insertion loss and high isolation, in comparison to those of corresponding semiconductor-based devices [1–3]. Therefore, RF-MEMS switches are expected to replace conventional semiconductor switches, especially in 5G transceiver modules [4]. Moreover, they are considered key devices in future satellite communication systems [5, 6]. However, RF-MEMS switches also have disadvantages that stem from their successive mechanical movement during ON–OFF switching. In particular, failure at contact points and self-actuation of ohmic contact type switches and capacitive type switches, respectively, are the main problems to be solved. In the case of ohmic contact type RF-MEMS switches, a failure in contacts are the most important factor limiting the devices' life time.

Many studies have been conducted to reduce contact failure rates. These studies have revealed several failure modes and causes related to contact failures. One of them, which is the contamination by materials such as carbon, oxygen and organic polymers [7, 8], is considered a major cause of failure. Therefore, minimizing contamination during the fabrication process and developing hermetic and reliable packaging to prevent contamination from the environment when the switch is working are important objectives. Another major cause of failure in contacts is the inherent characteristics of the contact materials. Numerous materials that improve the lifetime of RF-MEMS switch contacts have been proposed. Among them, we have focused on the carbon nanotube (CNT) dispersed Au electroplated layer of contacts. The CNT is considered a suitable material for electromechnical contact. Specifically, CNT-to-CNT contact was investigated to achieve a reliable MEMS switching devices [9, 10] and applied to inertial microswitch [11]. Moreover, the CNT has been reported to offer an advantage in terms of high-power handling capability [12]. In previous work, however, the uniformity of CNTs in the cantilever, including that of CNTs at the contact points, has been poor and uncontrollable. In previous studies, the contacts were formed by CNT dispersed Au electroplating. In this electroplating procedure, the CNTs must be dispersed well in the electroplating solution before

---

*Correspondence: sslee@tottori-u.ac.jp
[1] Graduate School of Engineering, Tottori University, Tottori, Japan
Full list of author information is available at the end of the article

electroplating is performed. However, because the CNTs exhibit high cohesion in the solution, preparing an electroplating solution, where the CNTs are stably dispersed for an extended period is difficult.

Herein, we propose a new method to fabricate Au/CNT-composite electroplated film to achieve a more reliable ohmic contact type RF-MEMS switch. In the fabrication procedure, we applied CNTs to the contact metal layer and formed an Au layer on then. Moreover, to reduce fabrication failure rate, we optimized the sacrificial metal layer etching process used in the fabrication. We designed, fabricated, and evaluated an RF-MEMS switch to demonstrate the proposed new fabrication method. The performance of the Au–Au/CNT contact RF-MEMS switch was compared with that of a conventional Au–Au contact RF-MEMS switch as well.

Method

Design

We designed a cantilever type electrostatically actuated RF-MEMS switch. A schematic view of the switch is shown in Fig. 1. It is an ohmic contact type single-pole single-throw (SPST) switch formed in a coplanar waveguide (CPW) configuration with ground (G)–signal (S)–ground (G) components. The characteristic impedances of the RF-MEMS switch and CPW were matched to 50 Ω.

In this study, we chose an ohmic contact type switch, which is less prone to damage from cosmic rays, because we expect the device to have aerospace applications [13]. Electrostatic force for cantilever actuation was applied via a separated actuation electrode fabricated below the cantilever. The separated actuation electrode is represented as the bias electrode in Fig. 1. Additionally, the bias resistor was connected in series to the actuation electrode to suppress the insertion loss when the switch was ON. At the same time, the bias resistor improved isolation when the switch was OFF. In a previous study, we demonstrated the effect of a bias resistor effect on RF characteristics [14]; specifically, for an Au–Au ohmic contacts type RF-MEMS switch, the insertion loss improved to 58% when the DC bias line resistance was increased approximately 7.3-fold.

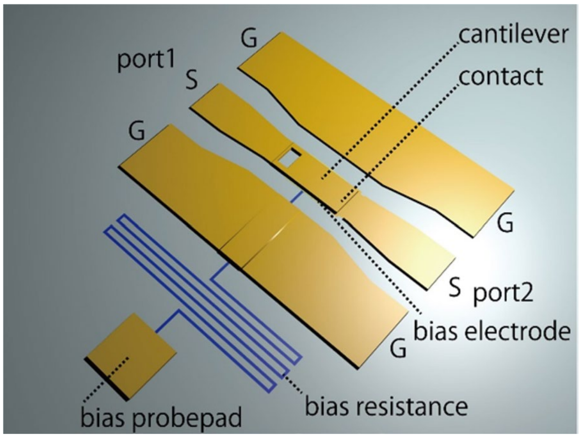

Fig. 1 A schematic view of the ohmic contact type RF-MEMS switch in coplanar waveguide configuration, which has ground (G)–signal (S)–ground (G) components

The Input and output ports are port1 and port2 in Fig. 1, respectively, and the pitch of the GSG probe is 150 μm. The dimensions of the cantilever were 60 μm × 150 μm, and its thickness was 5 μm. The cantilever was fabricated with an Au layer. The upper contact points were also formed with an Au layer on the cantilever. Two upper contact points were formed at the tip of the cantilever, and the contact point size was 2 μm × 2 μm. Although the upper contact points were fabricated with an Au layer owing to the ease of fabrication, the lower contact part was fabricated with the Au/CNTs-composite layer. To demonstrate the effectiveness of the Au/CNT lower contact layer, we also fabricated an RF-MEMS switch with an Au lower contact layer and compared its characteristics with those of the RF-MEMS switch with an Au/CNT lower contact layer.

The electrostatic force F_e generated through the actuation electrode to turn on the switch can be calculated via Eq. (1):

$$F_e = -\frac{1}{2}\frac{\varepsilon_0 W V^2}{g^2}, \tag{1}$$

where ε_0 is the dielectric constant, W is the area of the actuation electrode, g is the gap between the cantilever and the actuation electrode, and V is the applied voltage. However, the spring constant k of the cantilever is obtained via Eq. (2):

$$k = 3\frac{EI}{l^3}, \tag{2}$$

where E is the Young's modulus, I is the moment of inertia of the cantilever, and l is the length of the bending portion of the cantilever. The Young's modulus of Au is ~ 80 GPa. However, the Young's modulus of Au, which greatly affects the actuation voltage, depends on the crystal structure. The crystal structure of Au changes according to the conditions of electrolytic plating. Specifically, the Young's modulus varies depending on the film forming method and conditions; therefore, precisely determining the spring constant and the actuation voltage beforehand is difficult. Furthermore, according to the literature, the contact force for sufficient contact should be approximately 100–1000 μN [15]. Consequently, to achieve sufficient contact force, we set the actuation voltage applied to the switch to ~ 1.5 times the minimum drive voltage. In the experiment, the actual actuation voltage applied to the RF-MEMS switch was 90 V.

Fabrication

To fabricate the RF-MEMS switch having Au/CNT-composite contact as the lower contact, we first attempted to obtain a CNT layer by spraying CNTs onto the substrate. We then deposited an Au layer onto the sprayed CNT layer. To deposit the Au layer, two methods were used, sputtering and electroplating. We attained a stable layer using electroplating, and therefore used this method when fabricating the switch. The RF-MEMS switch was fabricated using surface micromachining. As Ni metal layer was used as a sacrificial layer to reduce organic material contamination during the fabrication process.

Fabrication of Au/CNTs composite layer

Prior to the fabrication of the RF-MEMS switch, we conducted basic experiments to achieve a stable Au/CNT-composite layer. During the deposition of the CNT containing layer, CNTs are easily agglomerated. Since CNTs are fibrous substance, they easily entangle with each other. Once they agglomerate, they cannot be released easily, and forming a uniform layer with agglomerated CNTs is extremely difficult. Therefore, the film containing CNTs must be kept in a released state, and the formation must be carried out while they are separated from each other. To avoid fabrication problems associated with CNT cohesion, we sprayed CNTs onto the lower contact Au layer. To spray the CNTs, we used a spray coater. The CNTs used for spray coating were prepared via the super-growth method [16] and were dispersed in an organic solvent using a homogenizer. When the CNTs are dispersed in a solvent, they can be chemically modified to exhibit hydrophilicity. Additionally, their dispersibility may be improved by adding a surfactant. However, when the CNT containing layer is used as the contact part in the switch, the aforementioned materials and modifications may contaminate the contacts and affect the devices' lifetime. During the fabrication process, we used an organic solvent composed mainly of *N,N*-dimethylformamide (DMF), which is volatile and eventually not retained. However, even with this method, maintaining the CNTs in a dispersed state for an extended period is difficult. Therefore, we repeated the process frequently using ultrasonic vibration for redispersion.

We applied the CNT coating by intermittently spraying a solution containing CNTs onto a Si substrate. The Si substrate was heated to 100 °C. Heating the Si substrate prevents the CNTs from agglomerating by rapidly evaporating the organic solvent. To obtain a stable CNT layer, we first sputtered an Au layer onto the CNT layer. However, after the Au film was sputtered, the CNT layer could not affix to the substrate. It was easily peeled from the Si substrate during the scratch test, as shown in Fig. 2. We next tested the electroplating method to deposit an Au layer to fix the sprayed CNT layer. We found that the CNT layer was securely formed on the Si substrate and that we could achieve a stable Au/CNT-composite layer. Moreover, we conducted O_2 reactive ion etching after electroplating to remove 1.5 μm thick photoresist for electroplating and the CNTs not to be formed into a composite film. Finally, we observed abnormally grown areas in the electroplated Au film. Their heights were taller than the gap between the cantilever and the lower electrode, which caused an electrical short between the cantilever and the lower contacts. To circumvent this problem, we attempted to flatten the lower contact layer using Ar ion milling.

Fabrication process of the RF-MEMS switch

The RF-MEMS switch with Au–Au/CNT-composite contacts was fabricated by surface micromachining on a high resistivity Si substrate. The fabrication process is described in Fig. 3.

First, as shown in Fig. 3a, on a high resistivity Si substrate (electrical resistivity: > 1 kΩ cm; diameter: 4 in.; thickness: 500 μm) with 1 μm thick thermal oxide film, the base metal layer composed of Ti/Au was deposited. The thicknesses of the Ti layer and the Au layer were 50 nm and 300 nm, respectively. The Ti layer functions as both an adhesion layer and a resistive bias line. We then formed the Au/CNT-composite layer as described in "Fabrication of Au/CNTs composite layer" section. The photoresist in Fig. 3a was prepared for Au electroplating on the sprayed CNT layer. The photoresist in Fig. 3a was then removed, and the base metal layers of Ti/Au were patterned. The Ti/Au layers were etched with the Ar ion

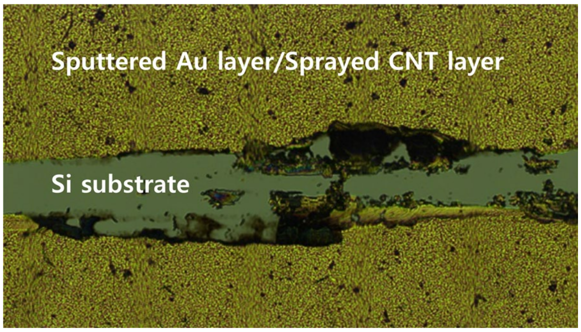

Fig. 2 The Au/CNT-composite layer composed of a sputtered Au layer and a sprayed CNT layer. The film was easily peeled from the Si substrate during scratch tests

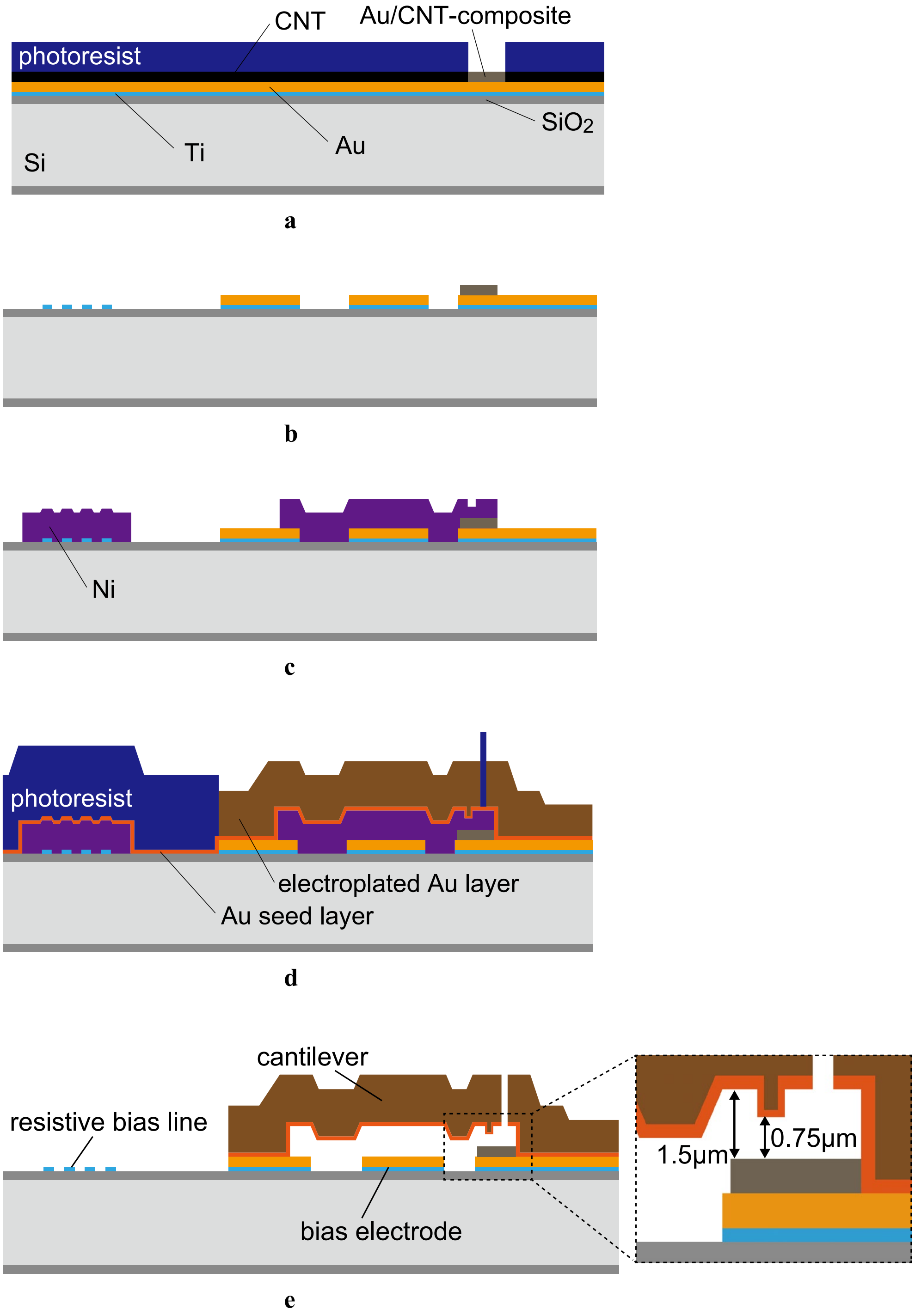

Fig. 3 Fabrication process of the RF-MEMS switch with Au–Au/CNT-composite contacts

beam etching (Ar IBE) technique. We then obtained the Ti resistive bias line after wet etching (etchant: AURUM-304) of the Au layer on the bias line (Fig. 3b). As shown in Fig. 3c, a 1.5 μm thick Ni sacrificial layer was deposited by sputtering and then etched using the Ar IBE method. We then successively formed 0.75 μm deep dimples for the formation of contact points under the cantilever; the dimples were also fabricated by the Ar IBE method.

The Au layer of the cantilever was formed by electroplating, as shown in Fig. 3d. Before electroplating, a 100 nm thick Au seed layer was sputtered and a photoresist (PMER P-LA900PM) for electroplating was patterned. The electroplated Au layer thickness was 5 μm. Finally, we removed the photoresist for electroplating and used Ar IBE to etch the part of the Au seed layer not involved in the formation of the Au electroplating layer. The Ni sacrificial layer was then removed. To prevent contamination by organic compounds, hydrochloric acid and ferric chloride, which are inorganic etchants, were used to etch the Ni layer. After the Ni sacrificial layer was etched, the solvent was replaced with isopropyl alcohol (IPA) and the CO_2 supercritical drying method was used to prevent stiction of the cantilever. In Fig. 3e, the fabricated switch is described. The gap between the cantilever body and the lower contact layer was 1.5 μm; however, the distance from the contact point surface formed on the cantilever to the lower electrode was 0.75 μm as shown in magnified of Fig. 3e.

The scanning electron microscopy (SEM) image of the fabricated RF-MEMS switch with Au–Au/CNTs contacts is shown in Fig. 4. In Fig. 4b, a magnified SEM image of Au/CNT-composite layer is shown; on the top surface, CNTs were observed fixed by the Au layer. During electroplating, Au grains were grown between CNTs vacant areas. The thickness of electroplated Au layer was set to slightly less than that of CNT layer to avoid completely embedding of CNT layer inside the Au layer.

Investigation and optimization of Ar ion beam etching process

In the fabrication process, Ar IBE method was used to etch metal layers except the Au layer etching on the Ti resistive line layer. The Ar IBE method is an anisotropic etching method, which can be applicable various metals because this method is using only an Ar ion bombardment onto the material. In the case of the Ar IBE method, the Ar ion beam incident angle is the most important process parameter and should be selected to reduce re-adhesion of etched metal onto the patterned photoresist side wall. The re-adhesion of etched metal forms a thin metal wall, which is difficult to remove and causes an electrical short.

In the Ar IBE process, we evaluated two Ar ion beam incident angles: 0° and 45°. The investigated Ar ion beam incident angle combinations for each metal layer etching process are summarized in Table 1.

In most of the RF-MEMS switches fabricated under the condition 1 in Table 1, we observed unintended leakage current. The leakage current was observed not only between signal lines in the OFF state but also between signal line and the actuation electrode pad, which should not normally conduct. Figure 5 shows an SEM image of the failed RF-MEMS switch cantilever area. An unintended substance was observed between the cantilever and the bias electrode. We performed wavelength-dispersive spectroscopy analysis to investigate the components of the undesired burr; the results are shown in Fig. 6. The undesired burr was confirmed

Table 1 Ar ion beam incident angles investigated in Ar IBE process

Condition	Base metal layer	Sacrificial layer	Dimple	Seed layer
1	0°	0°	0°	0°
2	45°	45°	45°	45°
3	45°	45°	45°	0°

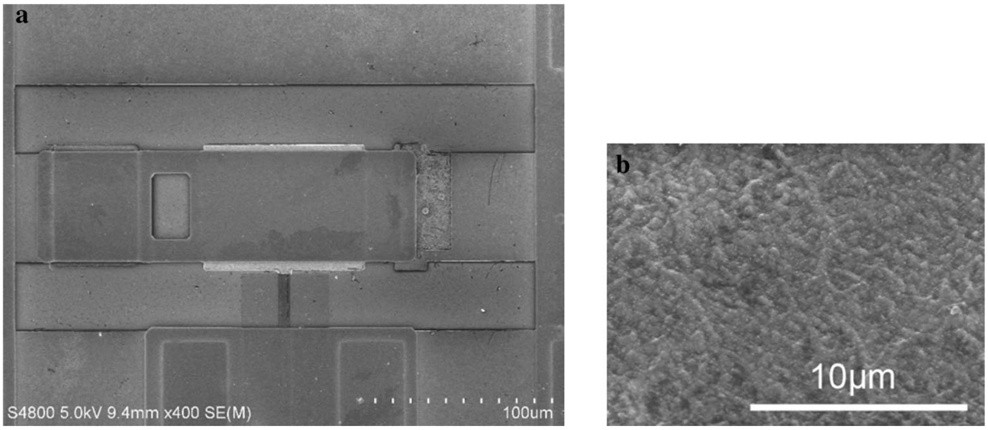

Fig. 4 SEM images of fabricated Au–Au/CNT-composite layer contact RF-MEMS switch: **a** a top-view of the switch, **b** a magnified view of the Au/CNT-composite layer

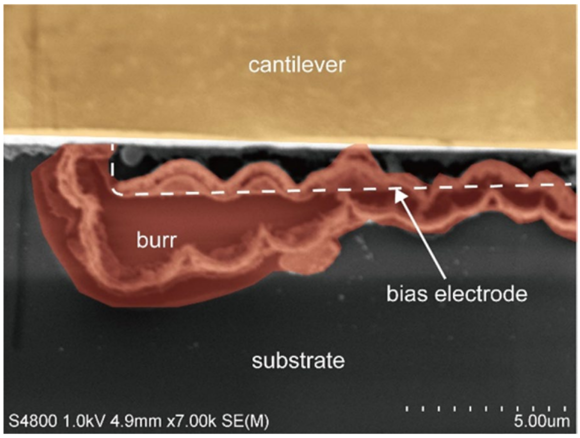

Fig. 5 SEM top-view image of the fabricated Au–Au/CNT-composite contacts RF-MEMS switch. For clarity, the cantilever and burr are colored

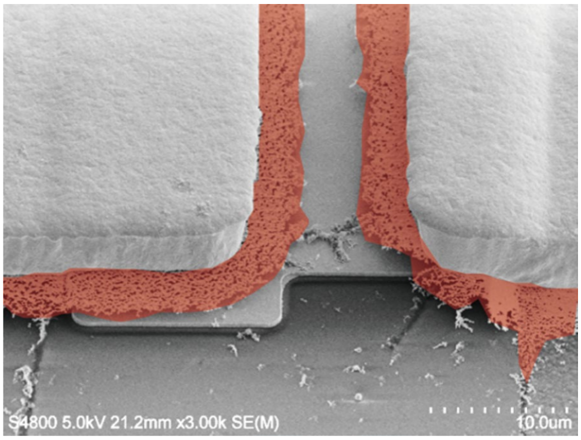

Fig. 7 SEM image of the remained Au seed layer after the Ar IBE process. For clarity, the remaining Au seed layer is colored red

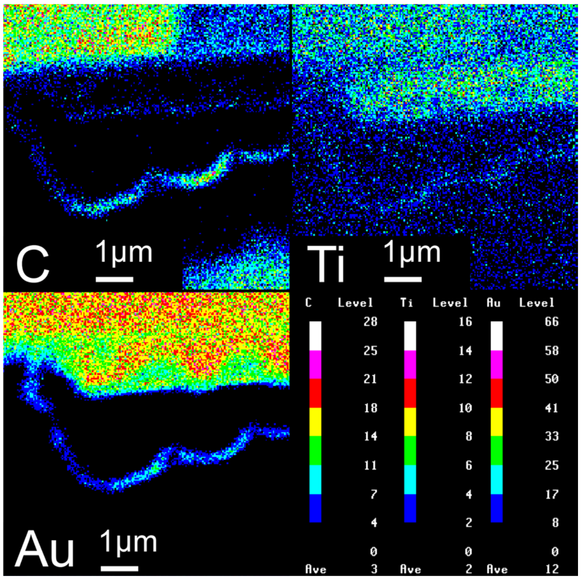

Fig. 6 Wavelength-dispersive spectroscopy analysis results for the unintended burr shown in Fig. 5

as Au and C. C is commonly observed and originated from the fabrication process material or from environmental air. Au, however, is speculated to have originated from the re-deposition of etched Au onto the photoresist side wall during etching of the base metal layer.

As a countermeasure, to suppress the re-deposition of etched Au onto the side wall of the photoresist, we changed the incident angle of the Ar ion beam onto the Si substrate to 45° in the Ar IBE process, which is condition 2 in Table 1. We expected that a 45° incident Ar ion beam bombardment of the side wall of the photoresist and the redeposited Au component would be removed. After fabricating a switch using a 45° incident Ar ion beam and evaluating the resulting device, we confirmed electrical isolation not only between signal lines but also between the signal line and actuation pad. Thus, a 45° angle of incidence of the Ar ion beam effectively prevented re-deposition of the etched Ar component onto the photoresist side wall. However, we observed an unetched Au seed layer beneath the electroplated Au layer, as shown in Fig. 7. This remaining Au seed layer can also lead to an electrical short. The remaining Au seed layer was caused by the thick electroplated Au layer. The thick electroplated Au layer acted as a barrier against the 45° incident Ar ion beam, and the Ar ion beam could not adequately impact the Au seed layer because of the shadow mask. To resolve this problem, we adjusted the angle of incidence of the Ar ion beam to 0° during the Au seed layer etching process. This modification is represented as condition 3 in Table 1. In the Au–Au/CNT contact RF-MEMS switch fabrication procedure, we applied condition 3 in Table 1 to the Ar IBE process. Consequently, we successfully fabricated RF-MEMS switches, as shown in Fig. 4.

Measurement results

We performed S-parameter measurements at frequencies up to 40 GHz to confirm the RF characteristics of the fabricated RF-MEMS switches with Au–Au/CNT-composite contacts. The S-parameter measurements were conducted with a vector network analyzer. The isolation and insertion loss are shown in Figs. 8 and 9, respectively. We achieved good isolation in the OFF-state. Furthermore, we achieved a low insertion loss of less

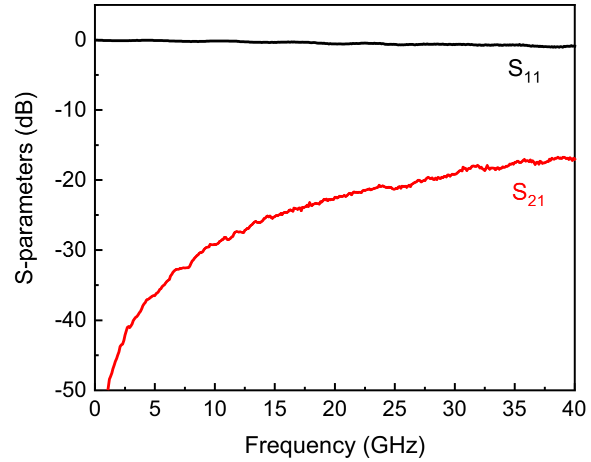

Fig. 8 Isolation characteristics of Au–Au/CNT-composite contact RF-MEMS switch in the OFF state

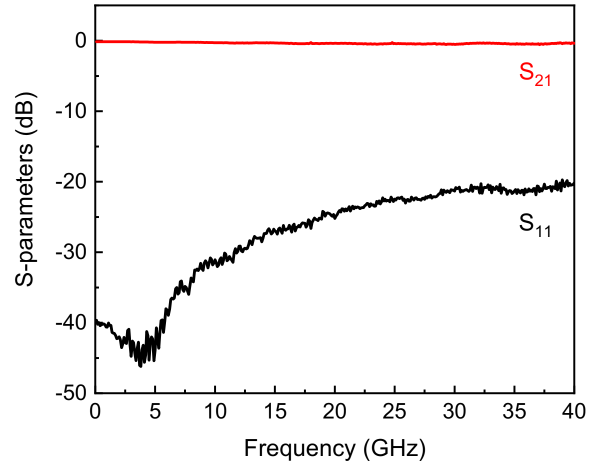

Fig. 9 Insertion loss of Au–Au/CNT-composite contact RF-MEMS switch in the ON state

than 0.7 dB at frequencies up to 40 GHz. We compared the insertion loss with that of an RF-MEMS switch with only Au–Au contacts, as shown in Fig. 10. As a result, we confirmed that the two devices exhibit similar insertion losses, although the insertion losses of the Au–Au/CNT-composite contact RF-MEMS switch are slightly higher than that of the Au–Au contact switch. This difference originates from the slightly higher resistivity of Au/CNT-composite layer compared with that of the Au layer. Furthermore, the life cycle of the Au–Au/CNT-composite contact switch was also evaluated. The life cycle test was performed by repeating the ON/OFF operations until the switch failed. The average number of cycles of the Au–Au/CNT-composite contact switch and Au–Au contact switch was ~ 9100 and ~ 3600 cycles, respectively.

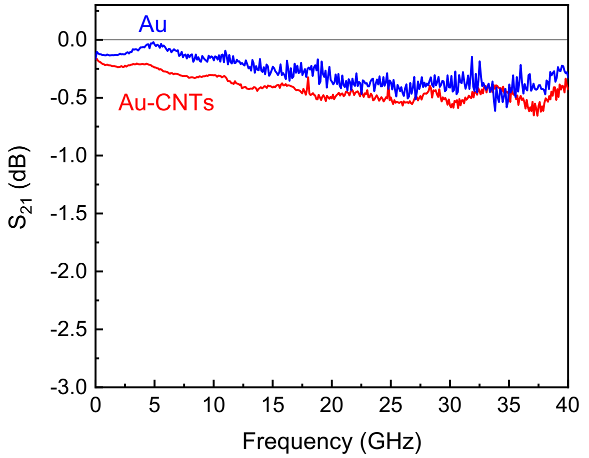

Fig. 10 Comparison of insertion losses between an RF-MEMS switches with Au–Au contacts and an RF-MEMS switch with Au–Au/CNT-composite contacts

These results suggest that we could achieve an RF-MEMS switch with a 2.7 times longer life cycle using Au/CNT-composite contacts.

Conclusions

Herein, we proposed a new fabrication method for Au/CNT-composite contacts to improve the reliability of ohmic contact type RF-MEMS switches. In the fabrication process, to prevent the CNTs from agglomerating, we sprayed the CNTs and then electroplated Au to fix the CNTs and obtain an Au/CNT-composite layer. Moreover, the Ar ion beam incident angle during the Ar IBE process for etching metal layers was investigated and optimized. We obtained deduced that a 45° Ar ion beam incidence angle led to the best result except in the case of etching the Au seed layer. For etching the Au seed layer, we deduced that the Ar ion beam incidence angle should be 0°. By applying both fabrication processes, we fabricated an RF-MEMS switch with Au–Au/CNT-composite contacts.

We performed S-parameter measurement and preliminary life cycle tests. The isolation was sufficiently high, and the insertion loss was less than 0.7 dB at frequencies up to 40 GHz. The Au–Au/CNT-composite contact RF-MEMS switch exhibited a longer life cycle than the Au–Au contact RF-MEMS switch. We demonstrated that the Au–Au/CNT-composite contacts can be considered a solution that improves the reliability and the high-power capability of ohmic contact type RF-MEMS switches. Improving the absolute number of life cycles, demonstrating the high-power capability, comparing results with other switches with different contact materials, and measuring switching speed will be considered as our future works.

Authors' contributions

SL and TK made substantial contributions to the conception, fabrication, measurement, summary, and drafting the manuscript. KS contributed to the conception and measurements, and LZ, JL, HT contributed to device fabrication. All authors read and approved the final manuscript.

Author details

[1] Graduate School of Engineering, Tottori University, Tottori, Japan. [2] Japan Aerospace Exploration Agency (JAXA), Tsukuba, Japan. [3] National Institute of Advanced Industrial Science and Technology (AIST), Tsukuba, Japan.

Acknowledgements

The authors would like to thank the CNT-Application Research Center, AIST, Japan and the Center for Integrated Nanotechnology Support, Tohoku University, Japan for their offer of CNTs and support for CNT coating technology, and for their support for a part of the fabrication technology, respectively.

Competing interests

The authors declare that they have no competing interests.

Funding

Funding information is not applicable.

Publisher's Note

Received: 13 October 2018 Accepted: 30 October 2018

References

1. Rebeiz GM (2003) RF MEMS: theory, design, and technology. Wiley, New York, pp 1–20
2. Patel CD, Rebeiz GM (2012) A high-reliability high-linearity high-power RF MEMS metal-contact switch for DC-40-GHz applications. IEEE Trans Microw Theory Tech 60:3096–3112
3. Rebeiz GM, Muldavin JB (2001) RF MEMS switches and switch circuits. IEEE Microwave Mag 2:59–71
4. Iannacci J (2018) RF-MEMS technology as an enabler of 5G: low-loss ohmic switch tested up to 110 GHz. Sens Actuat A 279:624–629
5. Ashok Kumar P, Girija Sravani K, Sailaja BVS, Vineetha KV, Guha K, Srinivasa Rao K (2018) Performance analysis of series: shunt configuration based RF MEMS switch for satellite communication applications. Microsyst Technol. https://doi.org/10.1007/s00542-018-3907-1
6. Kato M, Uchida O, Ichikawa F, Lee S-S (2014) Study of RF-MEMS switches for space application. In: Shin JK, Park J eds. The 7th Asia-Pacific conference on transducers and micro/nano technologies, Daegu, Korea, pp 1–2. CD-ROM, P1-94.pdf
7. Czaplewski D, Nordquist C, Dyck C, Patrizi G, Kraus G, Cowan W (2012) Lifetime limitations of ohmic, contacting RF MEMS switches with Au, Pt and Ir contact materials due to accumulation of 'friction polymer' on the contacts. J Micromech Microeng 22:105005
8. Newman HS, Ebel JL, Judy D, Maciel J (2008) Lifetime measurements on a high-reliability RF-MEMS contact switch. IEEE Microwave Wirel Compon Lett 18:100–102
9. Choi J, Lee J-I, Eun Y, Kim M-O, Kim J (2011) Aligned carbon nanotube arrays for degradation-resistant, intimate contact in micromechanical devices. Adv Mater 23:2231–2236
10. Choi J, Eun Y, Kim J (2014) Investigation of interfacial adhesion between the top ends of carbon nanotubes. Appl Mater Interfaces 6:6598–6605
11. Lee J-I, Song Y, Jung H, Choi J, Eun Y, Kim J (2012) Deformable carbon nanotube-contact pads for inertial microswitch to extend contact time. IEEE Trans Indus Electron 59:4914–4920
12. Izuo S, Yoshida Y, Soda S, Ogawa S, Lee S-S, Sakai Y, Fukumoto H (2010) RF-MEMS switch using carbon nanotube composite gold electroplating. IEEJ Trans SM 130:165–169
13. Ruan J, Papandreou E, Lamhamdi M, Koutsoureli M, Coccetti F, Pons P, Papaioannou G, Plana R (2008) Alpha particle radiation effects in RF MEMS capacitive switches. Microelectron Reliab 48:1241–1244
14. Kageyama T, Kato M, Miyashita H, Lee S-S (2016) Development of ohmic contact type RF MEMS switch and investigation of DC bias resistance influence on its RF characteristics. In: Sawada K ed. The 8th Asia-Pacific conference on transducers and micro/nano technologies, Kanazawa, Japan, pp 37–38. CD-ROM, 1b-5.pdf
15. Rebeiz GM, Patel CD, Han SK, Ko CH, Ho KMJ (2013) The search for a reliable MEMS switch. IEEE Microwave Mag 14:57–67
16. Hata K, Futaba D, Mizuno K, Namai T, Yumura M, Iijima S (2004) Water-assisted highly efficient synthesis of impurity-free single-walled carbon nanotubes. Science 306:1362–1364